

Supplementary Information

High-latitude obliquity forcing drives the Agulhas leakage

Thibaut Caley^{1,*}, Jung-Hyun Kim², Bruno Malaizé¹, Jacques Giraudeau¹, Thomas Laepple³, Nicolas Caillon⁴, Karine Charlier¹, Hélène Rebaubier⁴, Linda Rossignol¹, Isla S. Castañeda², Stefan Schouten² & Jaap S. Sinninghe Damsté²

1. Influence of factors other than temperature on SST proxies:

It is important to consider possible effects of factors other than temperature on the proxy records. For example, while TEX_{86} (former form of $\text{TEX}_{86}^{\text{H}}$) seems not to be affected by changes in salinity (Wuchter et al., 2004), it can be influenced by fluvial input of soil-derived isoprenoid GDGTs (Weijers et al., 2006). However, the Branched and Isoprenoid Tetraether (BIT) Index (Hopmans et al., 2004) provides a method to assess the relative amount of soil organic matter input. In sediments with high BIT Index values, it is likely that crenarchaeol and the other isoprenoid GDGTs are partially derived from soils (Weijers et al., 2006). Thus, it has been suggested that TEX_{86} only be applied in setting where the BIT Index is $\sim < 0.3$ (Weijers et al., 2006). In core MD96-2048, BIT values are extremely low (< 0.1 , Fig. S3D) indicating that the isoprenoid GDGTs have a predominantly marine source throughout the length of the record. Thus, an influence of fluvial input of soil-derived GDGTs on the TEX_{86} values at our core site can be excluded. Some studies have reported a seasonal bias on TEX_{86} or U_{37}^{K} records; however, this is likely not the case in the Mozambique Channel region. Although modern sediments have not been studied exactly at the site of MD96-2048, a nearby sediment trap study (16.8°S, 40.8°E; 2250 m water depth) (Fallet et al., 2010) provided some insights into application of these proxies in the Mozambique Channel, located upstream of site MD96-2048. At the Mozambique Channel sediment trap site, mean annual SST is 27.6°C, as measured by satellite remote sensing. The organic proxies were found to reflect mean annual SST but seasonal variability was not reflected in either TEX_{86} or U_{37}^{K} records or in fluxes of crenarchaeol or alkenones. In contrast, the Mg/Ca records were found to track seasonal variability in SST and shell fluxes of *G. ruber* were found to be strongly seasonal, peaking in late austral summer (March).

2. Lateral transport index:

Several early studies have noticed that U_{37}^{K} SST records are affected by laterally advected allochthonous input. For instance, Benthien and Müller (Benthien and Müller, 2000) showed that core-top U_{37}^{K} SSTs in the Argentine basin were affected by lateral advection of re-suspended sediments resulting in cold-biased U_{37}^{K} SST estimates. This lateral transport effect on U_{37}^{K} STs in the Argentine basin has been confirmed by more recent studies (Mollenhauer et al., 2006; Rühlemann and Butzin, 2006). Anomalously warm SSTs during the last glacial period were also observed in a marine sediment core recovered from the South East Indian Ridge (SEIR) at the location of the modern Subantarctic Front and attributed to a strong advection of detrital alkenones produced in warmer surface waters from the Agulhas region to SEIR (Sicre et al., 2005). More recently, Kim et al. (2009) also showed that U_{37}^{K} indicates much warmer SSTs during the last glacial period compared to all other SST estimates based

on diatom and foraminifera assemblages and TEX_{86} in the SEIR. These findings are consistent with core-top TEX_{86} data from the Argentine basin, recording no cold-biased SSTs in contrast to U_{37}^K SSTs (Kim et al., 2008). This is probably due to the rapid degradation of isoprenoid GDGTs compared to that of alkenones (Mollenhauer et al., 2008), which prevents GDGTs from being transported over long (>1000 km) distances. Furthermore, foraminiferal proxies have generally been shown to be least affected by lateral transport (Ohkouchi et al., 2002; Mollenhauer et al., 2008). Taken together, previous studies have shown TEX_{86} , modified now as TEX_{86}^H , and Mg/Ca of forams are less sensitive to the lateral transport than U_{37}^K . Because core MD96-2048 is located beneath the trajectory where the Agulhas current transports warm Indian Ocean toward the South Atlantic, we suspect a stronger lateral transport of alkenones than GDGTs, thus influencing the U_{37}^K record more than on the TEX_{86}^H record. Indeed, another core located southward of our study site and outside of the present Agulhas trajectory (MD96-2077) presents a distinctively different U_{37}^K SST signal. Therefore, we calculated SST differences (ΔSST) between U_{37}^K and TEX_{86}^H as well as between U_{37}^K and Mg/Ca for MD96-2048, as an indicator of the lateral transport from the Indian Ocean to the South Atlantic (Fig. S7). In general, both ΔSST records show higher values when the relative abundance of ALF (Peeters et al., 2004) decreases implying that lateral fluxes and thus the AC were stronger when Agulhas leakage was weaker. Consequently, our results provide an alternative hypothesis in contrast to the existing one that reduced glacial Agulhas leakage was caused by a weakened AC (Van Sebille et al., 2009).

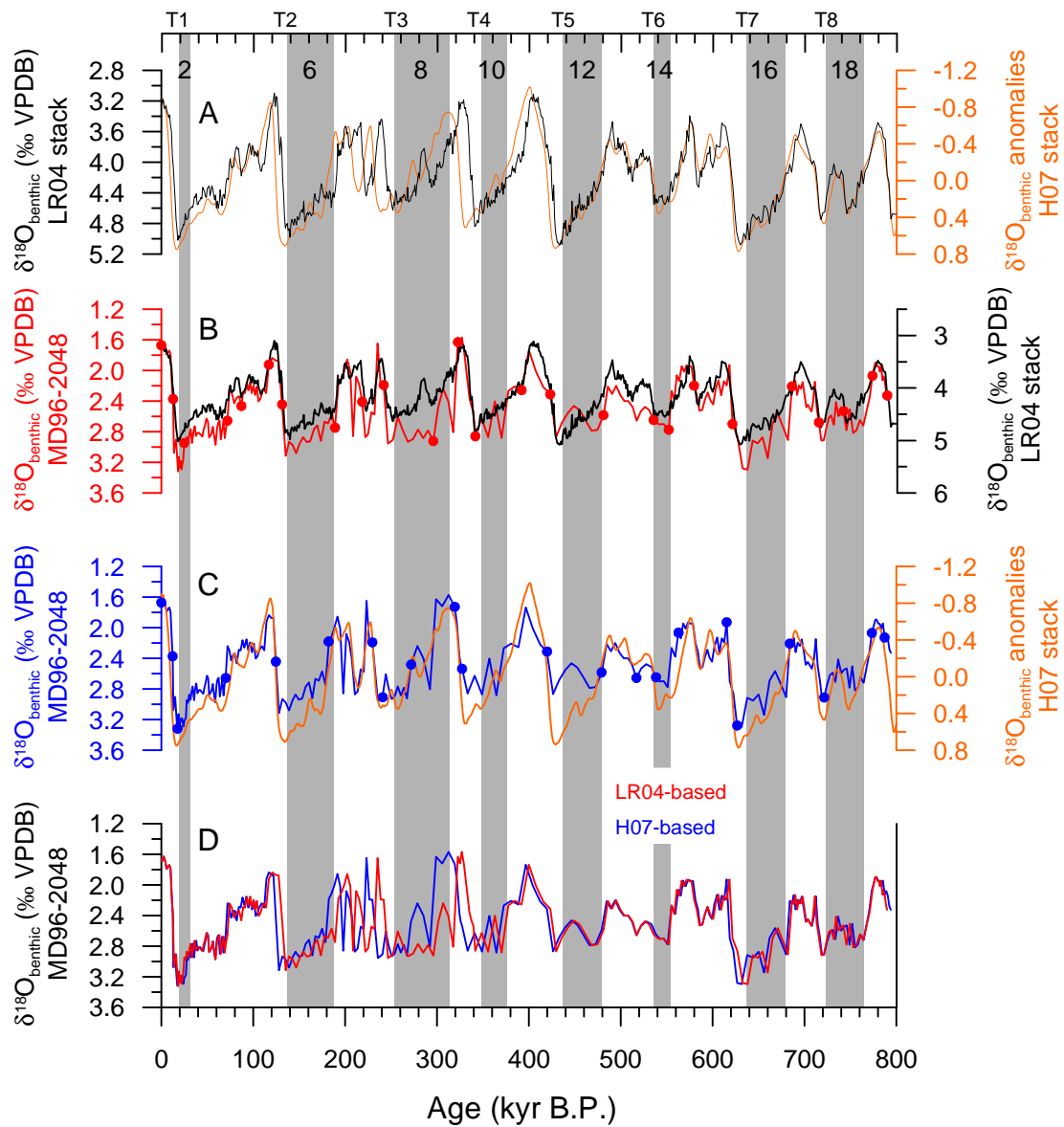


Fig. S1. A) Comparison of original stacks of LR04 (Lisiecki and raymo, 2005; black line) and H07 (Huybers, 2007; orange line). B) The $\delta^{18}\text{O}$ of the benthic foraminifer *P. wuellerstorfi* (red line) of core MD96-2048 after age tuning to the LR04 curve (black line) using the Analyseries software (Paillard et al., 1996). C) Similar to (B) but tuned to the H07 curve (orange line). D) Comparison of LR04- (red line) and H07-based (blue line) age models. Filled circles indicate the tie points of MD96-2048 $\delta^{18}\text{O}_{\text{benthic}}$ values to LR04 (Lisiecki and raymo, 2005; red) and H07 (Huybers, 2007; blue).

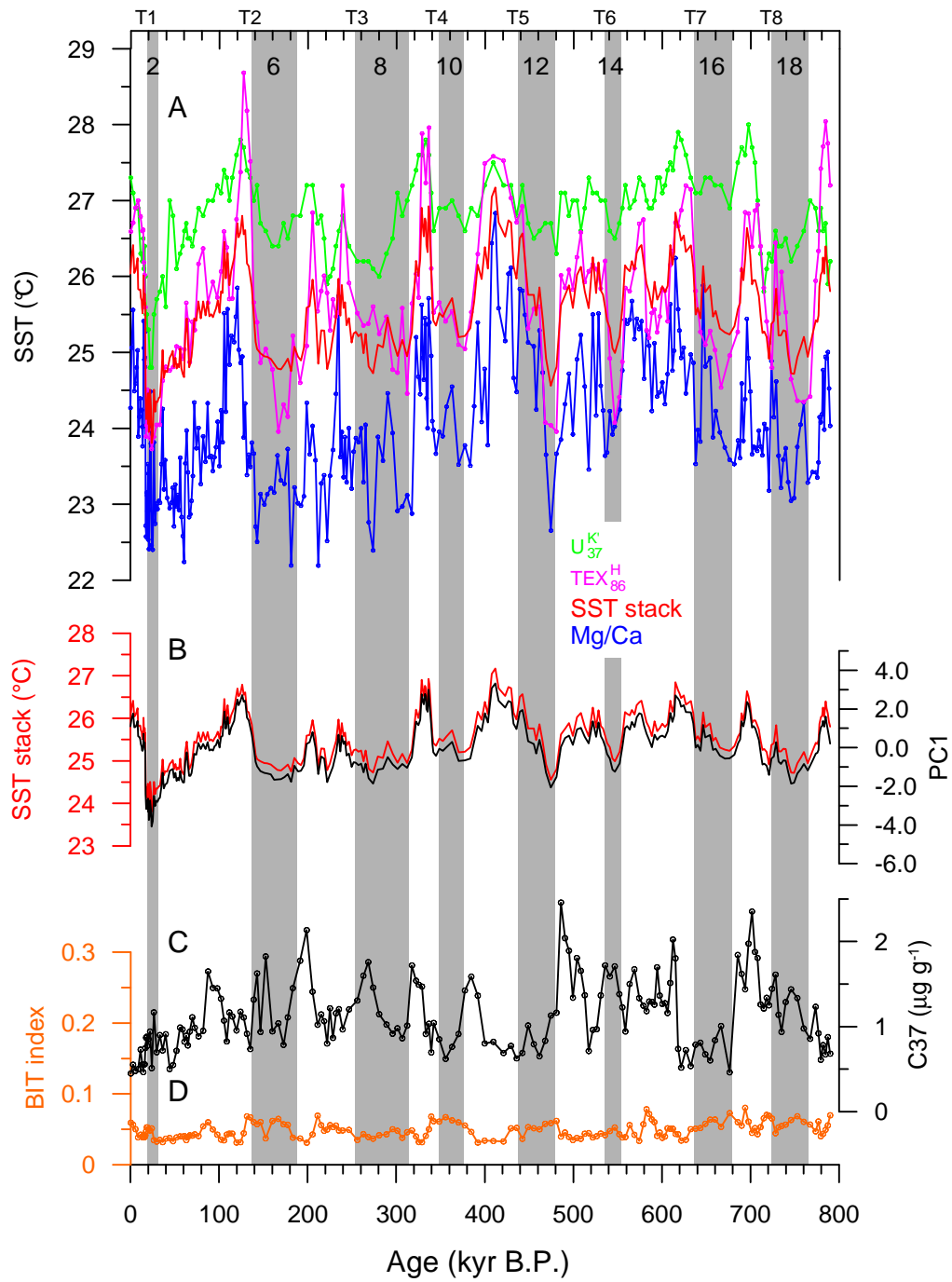


Fig. S2. Comparison of SST records from core MD96-2048. A) $U_{37}^{K'}$ (green line), TEX_{86}^H (purple line), Mg/Ca (blue line), and the SST stack (red line). B) Comparison of the SST stack (red line) with PC1. C) Alkenone concentrations (black line) and D) BIT index values (orange line).

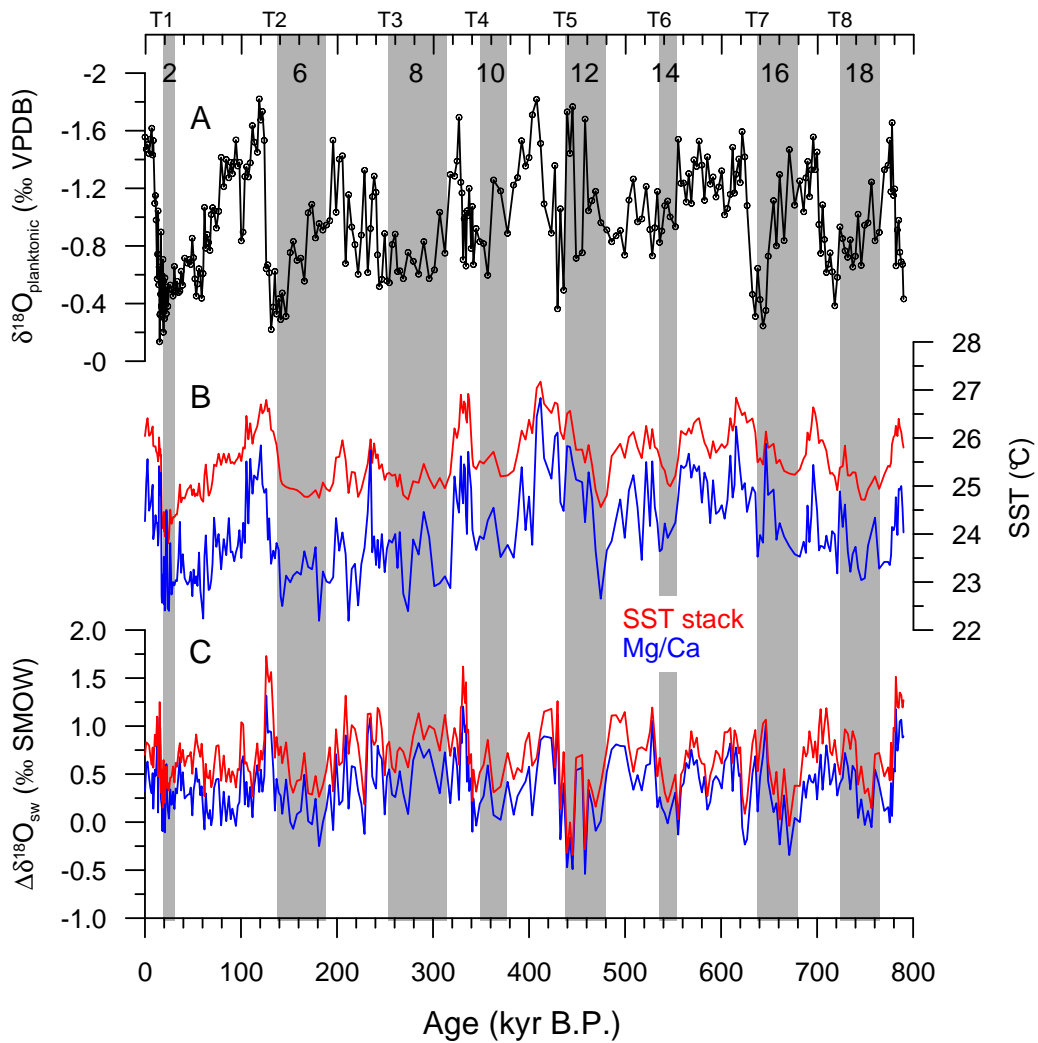


Fig. S3. Sea-surface salinity (SSS, $\Delta\delta^{18}\text{O}_{\text{sw}}$) reconstruction at core MD96-2048 following the method developed by Duplessy et al. (1991), which leans on the double influence of surface temperature and $\delta^{18}\text{O}$ isotopic composition of seawater ($\delta^{18}\text{O}_{\text{sw}}$) on the isotopic values of planktonic foraminifera. A) $\delta^{18}\text{O}$ measured in shells of the planktonic foraminifer *G. rubers.* s., B) the SST stack (red line) and Mg/Ca SST (blue line), and C) comparison of SSS reconstructions using the SST stack (red line) and Mg/Ca (blue line) records. We consider that the SST-Mg/Ca approach is, to date, the best tool for the SSS reconstruction because temperature and planktonic $\delta^{18}\text{O}$ records are based on the same material. However, both curves display the same variations.

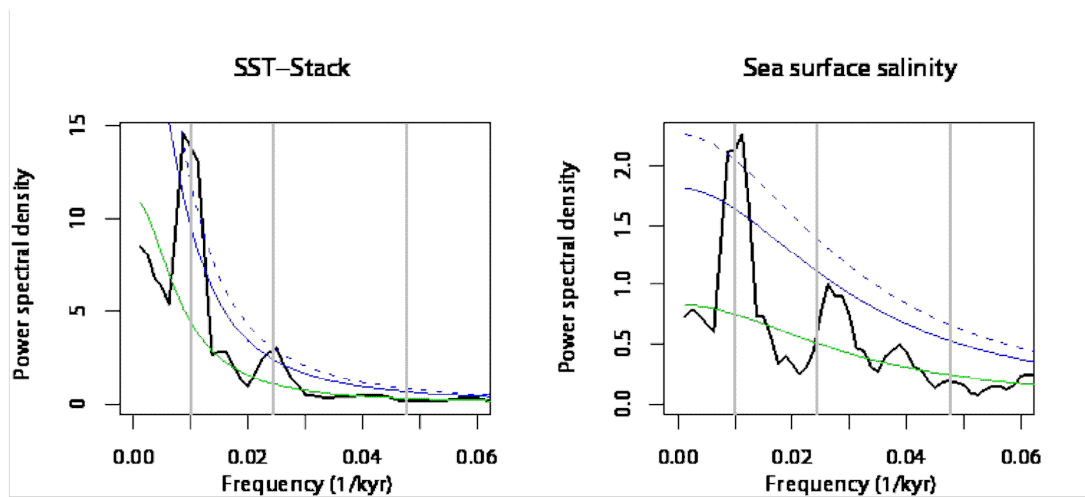


Fig. S4. Power spectrum of SST (top) and $\Delta\delta^{18}\text{O}_{\text{SW}}$ (bottom) using the alternative Huybers (2007) chronology. The spectrum is estimated using a smoothed periodogram. The spectrum background (green) and 95% (blue continuous) and 99% (blue dashed) confidence intervals are given. The orbital frequencies 1/100 kyr, 1/41 kyr and 1/21 kyr are marked with vertical grey lines.

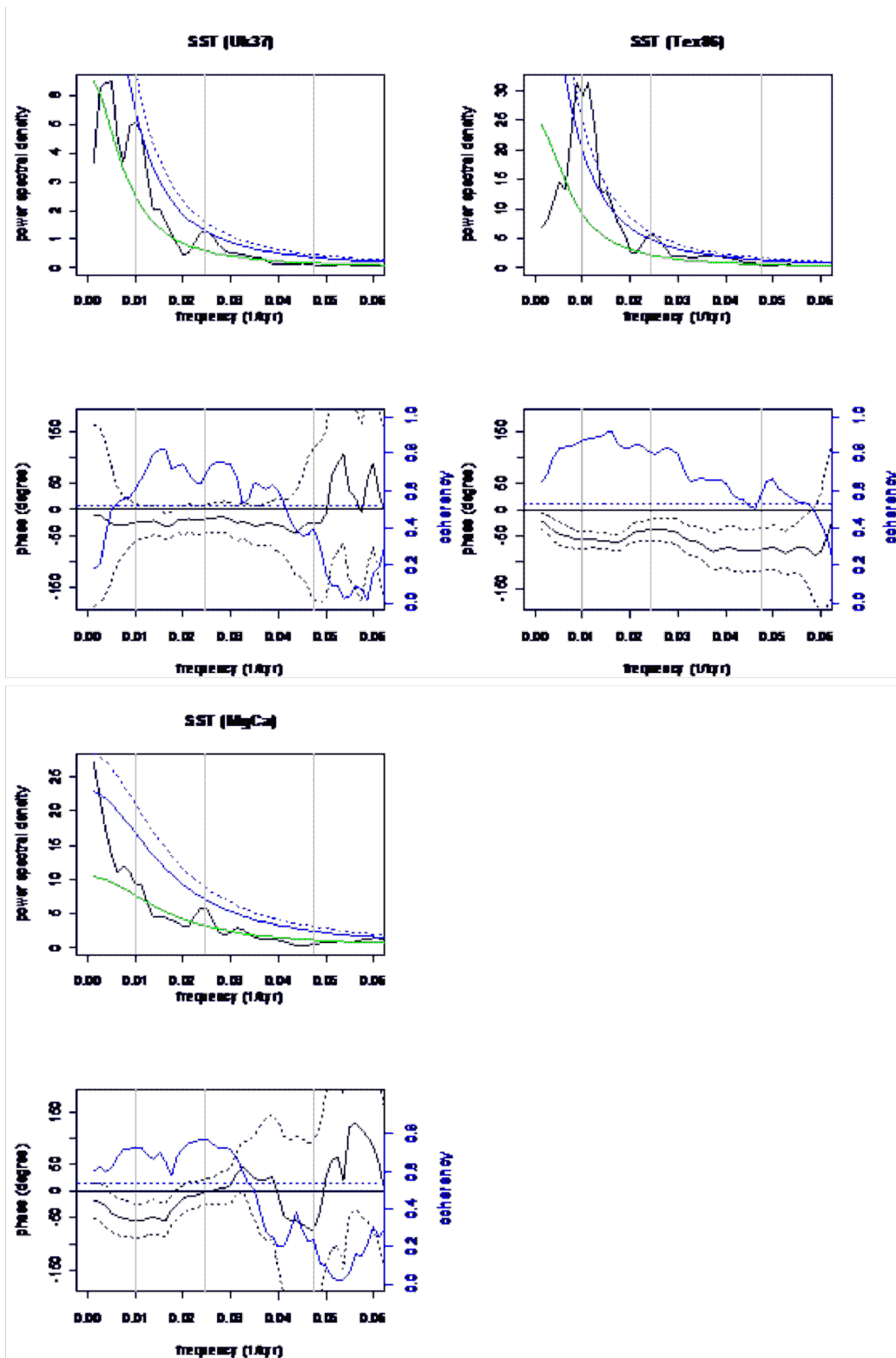


Fig. S5. Frequency spectra for separate Agulhas SST proxies and their coherence and phase relationship relative to global ice volume ($\delta^{18}\text{O}_{\text{benthic}}$) like Fig. 2. Upper panels: Power spectral density of SST (black line). A red noise background spectrum (green line) and 95% (blue continuous) and 99% (blue dashed line) confidence levels, relative to the red-noise background are given. Lower panels: coherence (blue line) and phase (black line) between the SST proxy and $-1 * \delta^{18}\text{O}_{\text{benthic}}$. The approximate 95% confidence level for the coherence (blue dashed line) and the 95% confidence interval for phase (black dashed line) are given. The orbital frequencies 1/100 kyr, 1/41 kyr and 1/21 kyr are marked with vertical grey lines. Both U_{37}^K and TEX_{86}^H show a time lag to $\delta^{18}\text{O}_{\text{benthic}}$ in the obliquity band. Mg/Ca seems to be in phase with the benthic $\delta^{18}\text{O}_{\text{benthic}}$.

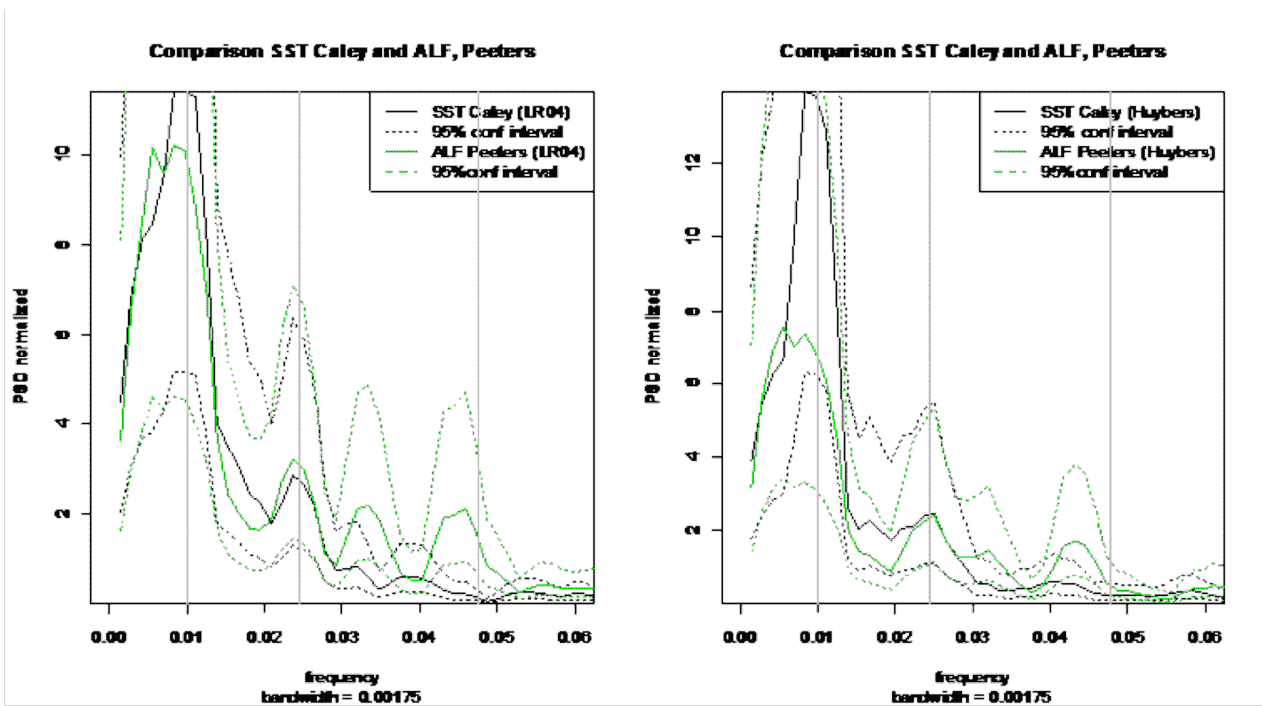


Fig. S6. Power spectrum of the ALF record (Peeters et al., 2004) using the newly established age models in this study. The ALF record is scaled to show the same power in the obliquity band as the SST stack record. The frequency band (1/100, 1/41 and 1/21kyr) are marked with grey vertical lines. One can clearly see that both spectra significantly differ in the precession band. The SST stack record shows no/very weak power in precession band, whereas the ALF record shows similar power as in the obliquity band. We can therefore reject the hypothesis that the presence of the precession band in the ALF record is caused by different tuning techniques.

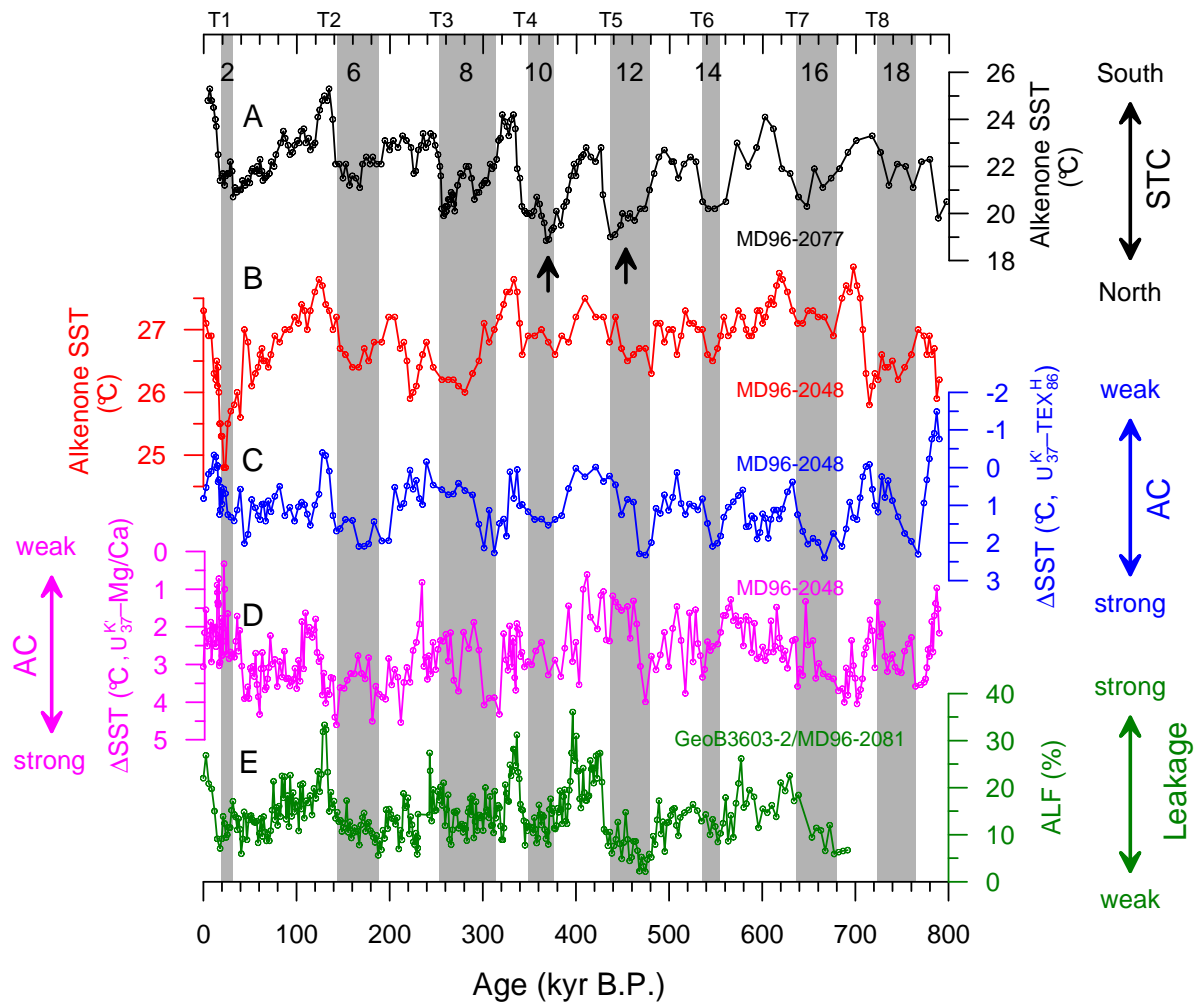


Fig. S7. Relationship between the subtropical convergence (STC) migration and the AC strength and transfer. A) $U_{37}^{K'}$ SST record of MD96-2077, which was used as a proxy of STC migration (Bard and Rickaby, 2009), B) $U_{37}^{K'}$ SST record at site MD96-2048. Warmer glacial SSTs were observed in our record when the STC reached its northern most position (black arrows), C-D) temperature differences (Δ SST) between $U_{37}^{K'}$ and TEX_{86}^H and between $U_{37}^{K'}$ and Mg/Ca obtained from MD96-2048 (see Supplementary Information), and E) Agulhas leakage fauna (ALF) record compiled from GeoB3603-2 and MD96-2081, a foraminiferal proxy of the Agulhas leakage (Peeters et al., 2004). Note that a new age model for GeoB3603-2 and MD96-2081 was built based on the correlation between the $\delta^{18}O$ of the benthic foraminifer and the LR04 stack (Lisiecki and Raymo, 2005) to allow comparison with our dataset. AC denotes the Agulhas Current.

Supplementary references

- Benthien, A. & Müller, P. J. Anomalously low alkenone temperatures caused by lateral particle and sediment transport in the Malvinas Current region, western Argentine Basin. *Deep-Sea Res. I* 47, 2369-2393 (2000).
- Fallet, U., Brummer, G. J., Zinke, J., Vogels, S. & Ridderinkhof, H. Contrasting seasonal fluxes of planktonic foraminifera and impacts on paleothermometry in the Mozambique Channel upstream of the Agulhas Current. *Paleoceanography* 25, doi:10.1029/2010PA001942 (2010).
- Hopmans, E. C. et al. A novel proxy for terrestrial organic matter in sediments based on branched and isoprenoid tetraether lipids. *Earth Plan. Sci. Lett.* 224, 107-116 (2004).
- Kim, J.-H. et al. Impact of lateral transport on organic proxies in the Southern Ocean. *Quat. Res.* 71, 246-250 (2009).
- Kim, J.-H., Schouten, S., Hopmans, E. C., Donner, B. & Sinninghe Damsté, J. S. Global sediment core-top calibration of the TEX₈₆ paleothermometer in the ocean. *Geochim. Cosmochim. Acta* 72, 1154-1173 (2008).
- Mollenhauer, G., Eglinton, T. I., Hopmans, E. C. & Sinninghe Damsté, J. S. A radiocarbon-based assessment of the preservation characteristics of crenarchaeol and alkenones from continental margin sediments. *Org. Geochem.* 39, 1039-1045 (2008).
- Mollenhauer, G., McManus, J. F., Benthien, A., Müller P. J. & Eglinton, T. I. Rapid lateral particle transport in the Argentine Basin: molecular ¹⁴C and ²³⁰Th_{xs} evidence. *Deep-Sea Res. I* 53, 1224-1243 (2006).
- Ohkouchi, N., Eglinton, T. I., Keigwin, L. D., & Hayes, J. M. Spatial and temporal offsets between proxy records in a sediment drift. *Science* 298, 1224-1227 (2002).
- Paillard, D., Labeyrie L. D. & Yiou, P. Macintosh program performs time-series analysis. *EOS Trans. AGU* 77, 379 (1996).
- Rühlemann, C. & Butzin, M. Alkenone temperature anomalies in the Brazil-Malvinas Confluence area caused by lateral advection of suspended particulate material. *Geochem. Geophys. Geosyst.* 7, doi:10.1029/2006GC001251 (2006).
- Sicre, M. A. et al. Mid-latitude Southern Indian Ocean response to Northern Hemisphere Heinrich events. *Earth Plan. Sci. Lett.* 240, 724-731 (2005).
- Wuchter, C., Schouten, S., Coolen, M. J. L. & Damste, J. S. S. Temperature-dependent variation in the distribution of tetraether membrane lipids of marine Crenarchaeota: Implications for TEX₈₆ paleothermometry. *Paleoceanography* 19 (2004).
- Weijers, J. W. H., Schouten, S., Spaargaren, O. C., Sinninghe Damsté, J. S. Occurrence and distribution of tetraether membrane lipids in soils: Implications for the use of the TEX₈₆ proxy and the BIT index. *Org. Geochem.* 37, 1680-1693 (2006).